

Research Article

Advancements in Green Fuel Technologies: The Synergistic Effect of Jatropha Biodiesel and Carbon Nanotubes on Diesel Engine Performance and Emissions

Muhammad Sarfraz Ali ,^{1,2} Shazia Noor ,³ Asad Naeem Shah,² Sadia Saleem ,⁴ Nasir Rafique ,² Muhammad Muzzammil Yasin ,⁵ Muhammad Faheem Nazar,² and Eustache Hakizimana ,⁶

¹Department of Transport Engineering, Faculty of Mechanical Engineering and Design, Kaunas University of Technology, Kaunas, Lithuania

²Department of Mechanical Engineering, University of Engineering and Technology, Lahore, Pakistan

³Department of Mechanical Engineering, Bahauddin Zakariya University, Multan, Pakistan

⁴Institute of CS and IT, The Women University, Multan, Pakistan

⁵Department of Mechanical Engineering, University of Management and Technology, Lahore, Pakistan

⁶Department of Mechanical and Energy Engineering, University of Rwanda, Kigali, Rwanda

Correspondence should be addressed to Shazia Noor; shazianoor@bzu.edu.pk and Eustache Hakizimana; haki2012eustache@gmail.com

Received 9 April 2025; Revised 29 October 2025; Accepted 6 November 2025

Guest Editor: Shikha Binwal

Copyright © 2025 Muhammad Sarfraz Ali et al. *Journal of Engineering* published by John Wiley & Sons Ltd. This is an open access article under the terms of the Creative Commons Attribution License, which permits use, distribution and reproduction in any medium, provided the original work is properly cited.

This experimental study investigates the impact of biodiesel derived from Jatropha oil and multiwalled carbon nanotubes (CNTs) on the performance and emissions of a diesel engine. The analysis involved five fuel conditions: pure diesel (D), diesel blended with 50% biodiesel (DB50), diesel blended with 80% biodiesel (DB80), diesel blended with 50% biodiesel and CNTs (DB50C), and diesel blended with 80% biodiesel and CNTs (DB80C). The results indicate that biodiesel blends, particularly those enhanced with CNTs, significantly improve fuel efficiency and engine performance. Blends with additives (DB50C and DB80C) exhibited higher brake power (BP) and lower brake-specific fuel consumption (BSFC) across various engine speeds, indicating more effective energy conversion and better fuel economy. Moreover, emissions analysis revealed that biodiesel blends with CNTs significantly reduce harmful emissions. Emissions of carbon monoxide (CO), unburned hydrocarbons (UHCs), and nitrogen oxide (NO_x) were consistently lower for DB50C and DB80C compared to D. The most notable reduction of 23.9% in NO_x emissions occurred at an engine speed of 2200, while CO and UHC emissions were reduced by 17.8% and 15.4%, respectively, at engine speeds of 1600 rpm. These findings suggest that the use of biodiesel with CNT additives not only increases combustion efficiency but also contributes to cleaner engine operation. This study emphasizes the potential of biodiesel, especially when combined with advanced nanoparticles, as a practical and environmentally friendly alternative to conventional diesel fuel.

Keywords: biodiesel; diesel engine; emissions; multiwalled carbon nanotubes; performance

1. Introduction

As global energy demand continues to rise, researchers are exploring alternative fuels to replace diesel in engines [1]. Diesel engines are preferred over other types due to their

cost-effectiveness, higher power output, and lower fuel consumption. Research is presently concentrated on hydrogen since it is a more eco-friendly fuel than fossil fuels, with better thermal efficiency and lower emissions [2, 3]. Table 1 shows the compilation of articles about emission control

TABLE 1: A compilation of articles about emission control strategies (the above and downward arrows represent a quantitative increase and decrease, respectively, in performance and emission parameters).

Sr. no.	Research group	Research work		Fuel additive	Engine performance				Engine emission			
		Base fuel			BSFC	BP	BT	BTE	NO _x	CO	UHC	Smoke
1	Celik et al. [4]	Diesel	Manganese	↓	↑	↑	—	—	↑	↓	↓	↓
2	Vellaiyan [5]	Diesel	Water emulsion	Improved	—	—	—	—	↓	↓	—	—
3	Wamankar and Murugan [6]	Diesel	Carbon black	—	—	—	—	—	↓	↑	↑	↑
4	Annamalai et al. [7]	Lemon and grass oil	Cerium oxide	—	—	—	—	↑	↓	↓	↓	↓
5	D'silva et al. [8]	Diesel	Titanium oxide	↓	—	—	—	↑	↑	↓	↓	—
6	Gumus et al. [9]	Diesel	Copper oxide	↓	↑	↑	—	—	↓	↓	↓	—
7	Hosseini et al. [10]	Diesel and biodiesel	Alumina	↑	↑	↑	—	↓	↑	↓	↓	—
8	Zhu et al. [11]	Diesel	Ferrous picrate	↑	↑	—	—	—	—	—	—	↓
9	Ali et al. [12]	Diesel and biodiesel	Carbon nanotubes	↓	↑	↑	↑	↑	↑	↓	↓	↓

strategies. The low autoignition temperature of biodiesel, which results in inappropriate engine combustion, was the main disadvantage of employing it. To address these limitations, fuels with lower autoignition temperatures are blended with hydrogen [13]. However, employing solid fuels, when they are used by blending them with pure diesel (D), results in increased fuel consumption and environmental harm. Based on the results of the earlier study, biodiesel showed promise as a green fuel substitute for H₂ in CI engines. Transesterification is a technique used to turn animal fats and both edible and inedible seeds into biodiesel [14].

The utilization of waste cooking oil from restaurants and households as a renewable fuel source has been widely explored. However, the high viscosity of oil derived from plants and seeds is typically lowered through a conventional two-stage transesterification process [15, 16]. It has been shown that the engine performs better overall when biodiesel is used, with increased torque, BTE, and brake-specific fuel consumption (BSFC). The peak temperature increases, and NO_x is created during combustion when there is more oxygen available [17]. A major challenge associated with the use of biodiesel is its impact on engine performance and emissions. Elevated NO_x emissions possess the capability to discharge supplementary greenhouse gases into the atmosphere, consequently potentially resulting in acid rain and smog [18].

Previous studies have demonstrated that waste coconut oil and fish oil serve as viable, low-cost feedstocks for biodiesel production, offering favorable fuel properties and reduced emissions compared to conventional diesel. Optimization of transesterification parameters, particularly catalyst concentration, reaction temperature, and methanol-to-oil ratio, has been shown to significantly enhance biodiesel yield, with nanocatalysts like MgO improving both conversion efficiency and reusability [19]. Another study shows that incorporating metal oxide nanoparticles such as MgO into biodiesel enhances engine performance and reduces harmful emissions by improving combustion efficiency and catalytic activity. However, limited research has focused on optimizing MgO nanoparticle concentrations in biodiesel blends derived from sustainable feedstocks like waste coconut and fish oils, which motivates the present investigation [20].

Biodiesel, derived from renewable sources such as vegetable oils and animal fats, is gaining recognition as a sustainable alternative to fossil fuels. Its use not only helps reduce reliance on nonrenewable energy sources but also contributes to environmental conservation. Research indicates that biodiesel combustion produces significantly lower emissions of carbon monoxide (CO), hydrocarbons (HCs), and smoke opacity than conventional diesel fuel. This reduction is primarily attributed to its oxygen-rich composition [21]. However, as a result of the higher combustion temperatures, biodiesel tends to produce higher nitrogen oxide (NO_x) emissions [22].

Blending a 30-ppm CeO₂ additive with diesel fuel significantly reduces emissions of NO_x, CO, smoke opacity, and HC compared to conventional diesel. This blend enhances engine performance by lowering NO_x emissions by 4.92% and smoke opacity by 11.82% compared to a standard biodiesel emulsion. Energy analysis suggests that this fuel mixture can serve as an alternative to conventional diesel, exhibiting lower energy losses (46.27%) and a higher energy utilization rate (53.73%) without requiring engine modifications. Kanimozhi et al. [23] examined the impact of blending karanja and safflower oil-based biodiesel with copper oxide (CuO) nanoparticles (50 ppm) at different biodiesel concentrations (20% and 40%) on engine performance and emissions. Their findings indicate optimal smoke reduction, NO_x control, and brake power (BP) output at an engine speed of 2100 rpm. The inclusion of CuO nanoparticles consistently enhances combustion efficiency and performance across various speeds. While karanja biodiesel exhibits better emission characteristics than safflower-based biodiesel, the addition of nanoparticles has only a minor effect on reducing combustion noise compared to pure biodiesel [24].

Gülüm [25] investigated the combined effects of compression ratio (CR), engine speed, and biodiesel blending ratio on the performance, emissions, and fuel cost of a diesel engine using corn oil biodiesel blends (B20, B40, and B60). The study revealed that moderate blends (e.g., B20) at lower CRs improved brake effective power and efficiency, while higher blends at higher CRs led to increased fuel consumption and reduced performance. Emission analysis showed that biodiesel blends significantly reduced CO, HC, and

smoke emissions, but increased CO_2 and NO_x . Furthermore, increasing the CR enhanced performance and reduced emissions across all fuels but raised the fuel cost due to the higher price of biodiesel. This comprehensive approach offers insight into optimizing engine parameters for biodiesel use.

Gaseous hydrogen-based fuels have many benefits, but they nevertheless face several difficulties. Ammonia addresses the challenges associated with storing and securing gaseous hydrogen while still providing the advantages of hydrogen due to its high hydrogen content [26]. Consequently, it functions as an intermediate fuel. While both methane and ammonia offer certain benefits, methane's carbon composition leads to CO_2 emissions in internal combustion engines, significantly contributing to carbon emissions. Stricter laws have been enacted in many nations to lower CO_2 emissions [27].

Gülmü [28] explored the impact of diesel-biodiesel-1-pentanol ternary blends on engine performance and exhaust gas temperature (EGT). The study showed that increasing the 1-pentanol content in blends led to reductions in brake effective power, peak cylinder pressure, and EGT, averaging up to 7.95% lower than conventional diesel. These effects were attributed to the lower calorific value, higher latent heat of evaporation, and higher viscosity of the ternary blends. Furthermore, the author developed predictive power and exponential models for EGT using engine operating parameters with high accuracy (average relative error below 3%). The findings underscore the role of higher alcohols like 1-pentanol in influencing combustion behavior and thermal performance in diesel engines.

Ammonia has attracted a lot of attention as a possible replacement for HC fuels since it overcomes the primary drawbacks of hydrogen and has a better power density, scalable infrastructure, and no carbon [29]. Ammonia favors the fuel properties since it can store and carry energy more efficiently than hydrogen. Its high-octane percentage makes it feasible to achieve a high CR, which boosts performance and reduces knocks. However, using pure ammonia in compression-ignition (CI) engines presents several challenges, including a high autoignition temperature, slow flame propagation, and a narrow combustion range. A promising approach to addressing these issues is dual-fueling ammonia with diesel in CI engines. Under standard conditions of room temperature and a pressure of 10 bar, ammonia can be rapidly liquefied and offers a volumetric power density approximately 1.8 times higher than that of liquefied hydrogen [30].

Recent studies have explored ternary blends of diesel, biodiesel (corn oil), and higher alcohols like 1-pentanol to evaluate their impact on engine performance and emissions. A regression model and its Fourier series representation were used to estimate in-cylinder pressure data. The study reported that ternary blends reduced CO (up to 13.15%), HC (up to 36.25%), and smoke emissions (up to 7.41%) while slightly increasing NO_x emissions. Additionally, these blends exhibited shorter combustion duration, longer ignition delay, and lower brake effective efficiency compared to D. These findings underline the emission-reducing potential of alcohol-diesel-biodiesel blends in compression ignition engines [31].

Recent studies have explored biodiesel blends enhanced with metal oxide nanoparticles to improve combustion efficiency and reduce emissions. However, most existing works rely on one-variable or linear optimization methods like RSM, which fail to capture the complex nonlinear interactions in engine systems. To address this, hybrid metaheuristic approaches such as the RSM-Rao algorithm have emerged as promising tools for optimizing biodiesel-fueled CI engine performance and emission control [32].

Recent advancements in alternative fuel additives have highlighted the potential of nanomaterials such as carbon nanotubes (CNTs) to improve fuel performance and emission characteristics in diesel engines. CNTs, due to their unique chemical and physical properties, act as effective combustion catalysts, promoting more complete and efficient combustion processes. This leads to notable enhancements in engine performance parameters, including BP and BSFC, while also minimizing harmful emissions such as CO, NO_x , and particulate matter (PM) [33]. Furthermore, their application in biodiesel-diesel blends addresses challenges such as poor oxidative stability and lower calorific value, making CNTs a promising additive for sustainable fuel applications. Previous studies have demonstrated the efficacy of CNTs in reducing frictional losses, enhancing thermal stability, and providing better spray atomization in compression ignition engines. The exhaust emissions and performance of the diesel engine have been evaluated by numerous prior researchers using carbon nanotubes and biodiesel mixed with D [34]. Carbon nanotubes have been shown to improve engine performance in D while reducing exhaust emissions from diesel engines. Recent years have seen a large number of studies on emissions and engine performance, with a focus on nanofuel additives. On the other hand, there are still a lot of unanswered issues about how blended D and CNTs affect the emissions and performance characteristics of diesel engines.

While previous studies have individually explored the use of biodiesel or nanomaterials like CNTs to enhance diesel engine performance and emissions, there remains limited research on the synergistic effect of combining biodiesel derived from Jatropha oil with multiwalled carbon nanotubes (MWCNTs) at varying concentrations in diesel blends. This study uniquely examines the integrated impact of two sustainable fuel technologies, that is, biodiesel and CNTs, on performance metrics such as BP and BSFC, as well as emissions including CO, NO_x , and UHC. Figure 1 illustrates the flowchart of the current experimental study. By systematically testing blends with 50% and 80% biodiesel along with CNT concentrations, the research provides a comprehensive understanding of their combined influence, which is largely underexplored in current literature. Furthermore, the study uses statistical validation to confirm the significance of the observed trends, offering a data-driven assessment that reinforces the novelty of its findings.

2. Experimental Setup

2.1. Preparation of Test Fuel. A structured methodology was employed to prepare the test fuel for an experimental study

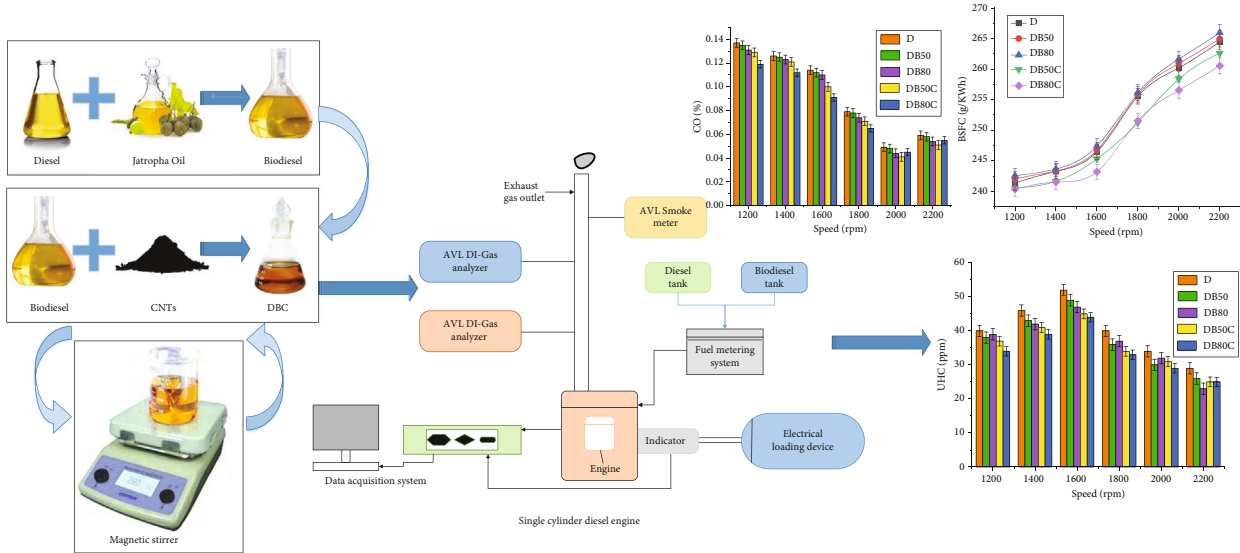


FIGURE 1: Flowchart of the current experimental study.

examining the effects of biodiesel and nanoparticles on diesel engine performance and emissions. The necessary materials were procured from reliable sources, with diesel fuel and Jatropha oil obtained from Pakistan State Oil, while CNTs were imported from China. The biodiesel was synthesized through the transesterification of Jatropha oil. This process involved heating the oil to 60°C and mixing it with methanol in the presence of a potassium hydroxide catalyst. The reaction led to the production of methyl esters (biodiesel) and glycerol. The mixture was continuously stirred for 1–2 h before being left to settle, allowing the biodiesel to separate from the glycerol.

The CNTs used in this study were characterized prior to blending. TEM and BET analyses confirmed that the CNTs exhibited a multiwalled tubular morphology, consisting of several concentric graphene layers. The average outer diameter was in the range of 12–15 nm, with a length of 3–15 μm and a purity level of approximately 97%, as listed in Table 2. The BET surface area was measured between 50 and 270 m^2/g , consistent with the porous and high aspect ratio structure typical of MWCNTs. Figure 2 shows the SEM image of the CNTs, demonstrating their uniform tubular morphology and minimal agglomeration. These characteristics confirm that the CNTs used were MWCNTs, which provide enhanced surface reactivity and catalytic properties when dispersed in the biodiesel–diesel blends.

Next, biodiesel–diesel blends were prepared. For instance, to create a 50% biodiesel–diesel blend (DB50), 50 mL of biodiesel was added to 1-L diesel and thoroughly mixed using a high-shear mixer. To enhance the fuel properties, CNTs were incorporated into these blends. The concentration of CNTs was determined based on desired enhancement levels, such as 50 ppm. In this study, the CNT concentration of 50 ppm represents a mass-based concentration, corresponding to 50 mg of CNTs per kilogram of the biodiesel–diesel fuel blend. The dispersion of CNTs involved weighing the required amount using precision scales, adding them to the biodiesel–diesel blend, and using

TABLE 2: Specifications of carbon nanotubes.

Item	Specification
Length	3 ~15 μm
Diameter	12~15 nm
Purity	97%
Ash content	< 2.5%
Specific surface area	50~270 m^2/g
Bulk density	0.06~0.09 g/cm^3

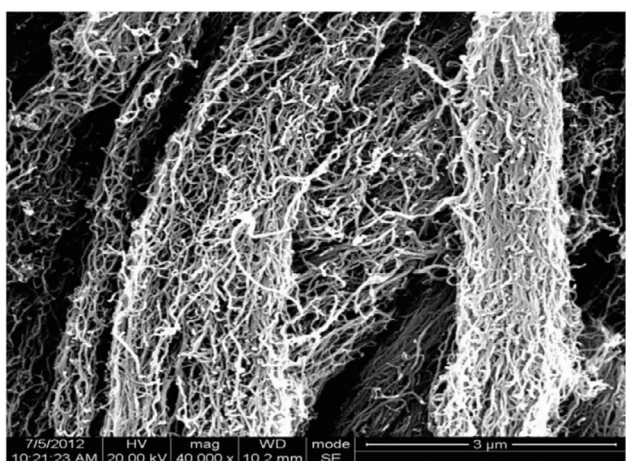


FIGURE 2: SEM photograph of CNTs.

an ultrasonic homogenizer to achieve uniform dispersion. This process typically required 30–60 min to ensure the CNTs were evenly distributed without agglomeration. The design of the experiment is presented in Table 3.

The prepared fuel blends were then stored in clean, sealed containers to prevent contamination and evaporation. Stability testing was performed to verify the consistent

TABLE 3: Design of experiment.

Name	Diesel (%)	Biodiesel (mL)	CNTs (ppm)
D	100	0	0
DB50	100	50	0
DB80	100	80	0
DB50C	100	50	50
DB80C	100	80	50

dispersion of CNTs and the long-term homogeneity of biodiesel–diesel blends, using periodic visual assessments and analytical methods such as particle size analysis. Quality control tests were performed to verify the properties of the prepared fuel blends, ensuring they met the necessary specifications for use in diesel engines. Key properties tested included flash point, cetane number, calorific value, viscosity, and density. This comprehensive preparation process ensured the test fuels were suitable for evaluating the impact of biodiesel and nanoparticles on diesel engine emissions and performance.

The dispersion of CNTs in the biodiesel–diesel matrix was achieved using a probe-type ultrasonic homogenizer (250 W, 20 kHz) for 45 min at a controlled temperature of $30^{\circ}\text{C} \pm 2^{\circ}\text{C}$ to prevent overheating. To enhance dispersion stability and minimize nanoparticle agglomeration, 0.1 wt% of cetyltrimethylammonium bromide (CTAB) was used as a surfactant. The prepared blends were allowed to stabilize for 24 h before testing to ensure uniform distribution.

The stability of the nanofuels was evaluated through visual observation, UV–Vis spectrophotometry, particle size analysis, and zeta potential measurements. The UV–Vis absorbance spectra were recorded in the range of 200–800 nm, showing no significant change in absorbance intensity over 21 days, indicating high stability. The average particle size of the dispersed CNTs was approximately 45 nm, while the zeta potential value of -38.6 mV confirmed electrostatic repulsion sufficient to prevent aggregation. Sedimentation tests, demonstrated negligible settling for up to 21 days. The blends remained visually homogeneous for nearly 3 weeks before testing, confirming satisfactory stability for engine experiments.

Agglomeration can potentially influence the combustion process by affecting atomization quality and local heat release; however, due to the optimized sonication energy, controlled temperature, and surfactant-assisted stabilization used in this study, the CNTs remained well dispersed throughout the test duration, ensuring consistent and reproducible combustion behavior.

2.2. Experimental Setup and Operating Conditions. The experimental setup is meticulously designed to assess how biodiesel and nanoparticles influence diesel engine performance and emissions, ensuring accurate and comprehensive data collection. The core of the setup is the diesel engine, where test fuels are combusted. Fuel supply is managed by separate tanks for diesel and biodiesel, both sourced from Pakistan State Oil, with the biodiesel blended with CNTs

imported from China. The fuel metering system ensured accurate fuel injection rates, maintaining consistent engine operation. Figure 3 depicts the schematic diagram of the experimental setup.

To simulate practical conditions, an electrical loading device is connected to the engine, allowing for the application of variable electrical loads. Engine performance parameters such as speed, torque, BSFC, and power output were observed by an indicator. The EGT is continuously measured using thermocouples, providing data on thermal efficiency and combustion stability.

Emission analysis is an essential aspect of the system. An AVL DI-Gas analyzer is used to measure exhaust gas components such as CO, NO_x , and unburned hydrocarbons (UHCs). Additionally, an AVL smoke meter quantifies smoke opacity, indicating PM emissions. All performance and emission data are captured by a data acquisition system, which interfaces with various sensors and analyzers to record and process the results.

Experiments are conducted under controlled conditions, with engine speeds ranging from 1200 to 2200 rpm and varying loads to simulate different driving scenarios. The exhaust temperature and emissions are monitored throughout, ensuring stable combustion and accurate data collection. The data acquisition system logs all relevant parameters, including fuel consumption, engine power, exhaust temperature, and emission concentrations. The comprehensive experimental setup, utilizing advanced measurement equipment and consistent operating conditions, enables a thorough investigation into how biodiesel and nanoparticles affect diesel engine performance and emissions. The collected data provide valuable insights into the viability of biodiesel and nanoparticle blends as alternative fuels, highlighting their potential benefits and drawbacks.

To ensure repeatability and statistical reliability, each experimental test was conducted three times under identical operating conditions for every fuel blend. The average of the three readings was reported for each performance and emission parameter, while the standard deviation ($\pm\text{SD}$) was calculated to represent the variability among repeated trials. All graphical data (Figures 4, 5, 6, 7, and 8) include error bars indicating $\pm\text{SD}$ values. The inclusion of these error bars provides a quantitative representation of measurement precision and ensures that differences observed among fuel blends (e.g., 50% biodiesel–diesel blend with an additive (DB50C) vs. DB50) are statistically meaningful.

2.3. Uncertainty Analysis. To ensure the accuracy of the computed characteristics, it is crucial to evaluate the associated uncertainty. Equation (1) determines the total uncertainty by analyzing the propagation of individual measurement uncertainties, following the standard uncertainty analysis methodology. Uncertainty refers to the range of variation in repeated measurements, whereas accuracy indicates how closely a measurement aligns with the true value.

To calculate the overall uncertainty, the root-sum-square (RSS) method was applied according to the standard propagation of uncertainty principle:

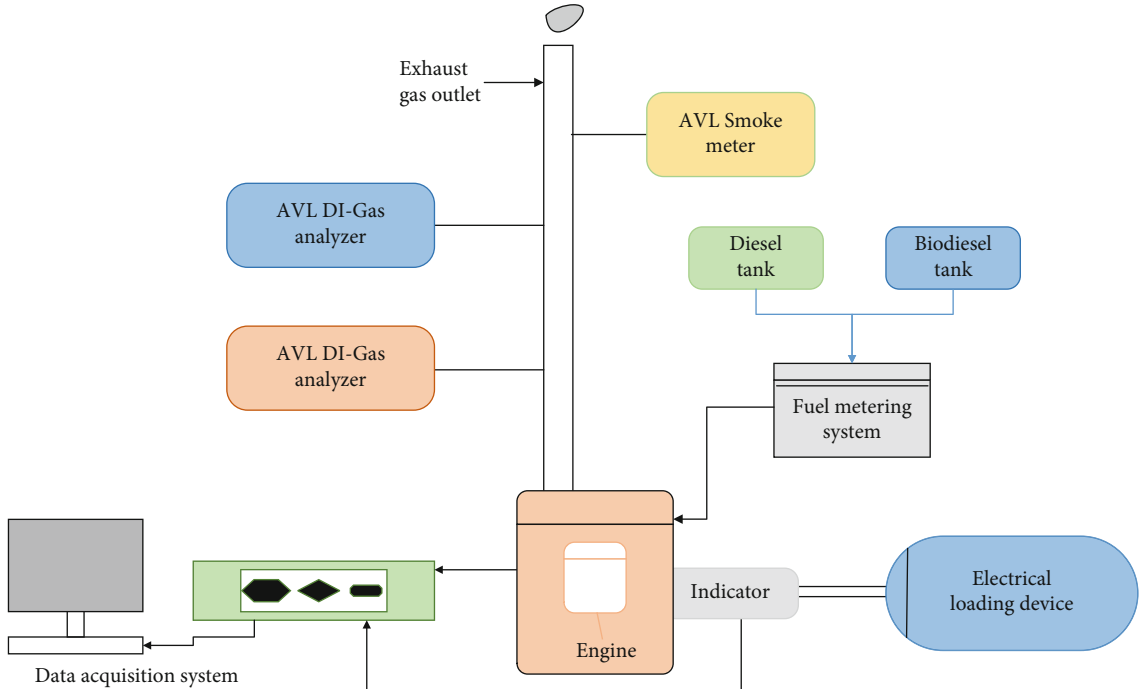
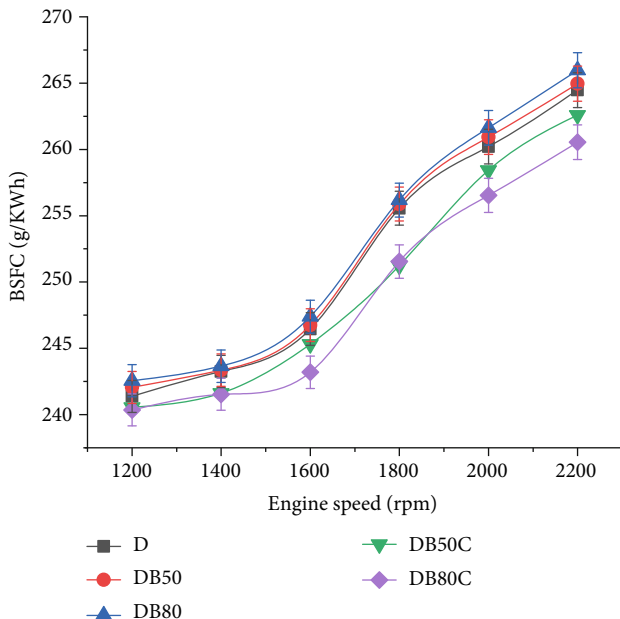
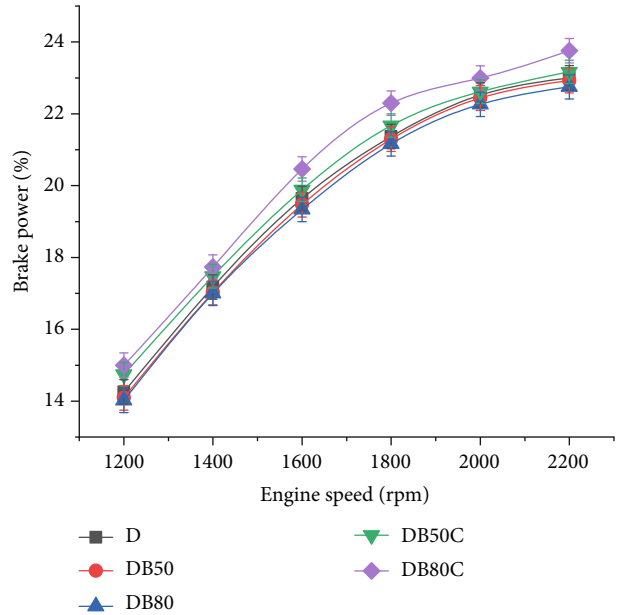


FIGURE 3: Schematic diagram of the experimental study.

FIGURE 4: Brake-specific fuel consumption across various engine speeds (error bars represent the standard deviation ($\pm SD$) based on three repeated experimental trials under identical conditions).

$$\omega Y = \sqrt{\sum_{i=1}^n \left(\frac{\partial Y}{\partial X_i} \omega X_i \right)^2}, \quad (1)$$

where ωY is the overall uncertainty in the derived quantity Y (e.g., BSFC or BP), and ωX_i represents the individual uncertainty in each measured parameter X_i . The uncertainties of

FIGURE 5: Brake power across various engine speeds (Error bars represent the standard deviation ($\pm SD$) based on three repeated experimental trials under identical conditions).

all independent measurements, such as load, speed, fuel consumption, EGT, and emission readings, were combined through this relation.

For parameters measured directly by instruments (e.g., speed, temperature, and gas concentrations), the manufacturer-specified accuracies were used. For calculated parameters like BP and BSFC, the uncertainties were propagated using the above equation. Specifically,

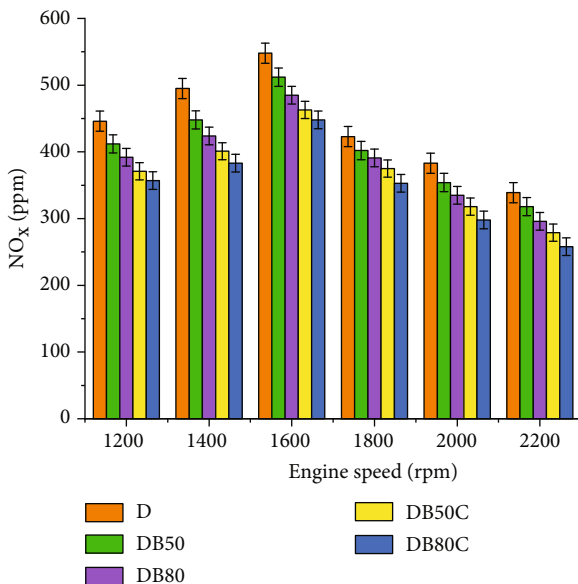


FIGURE 6: NO_x emissions across various engine speeds (error bars represent the standard deviation ($\pm\text{SD}$) based on three repeated experimental trials under identical conditions).

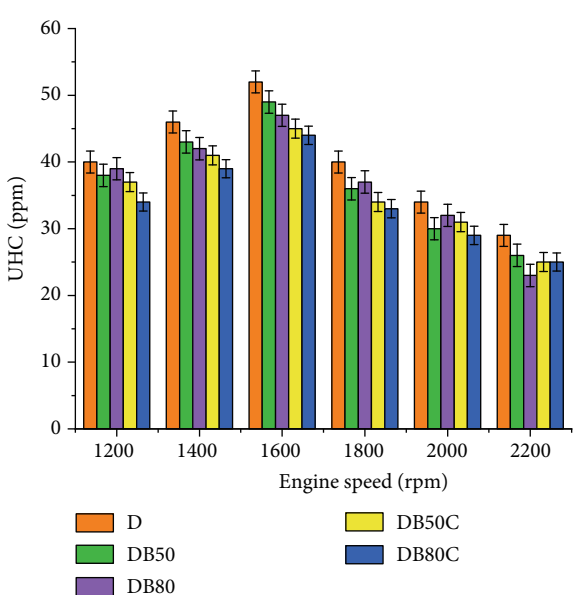


FIGURE 7: UHC across various engine speeds (error bars represent the standard deviation ($\pm\text{SD}$) based on three repeated experimental trials under identical conditions).

$$\text{BSFC} = \frac{\dot{m}_f}{P_b}.$$

The uncertainty in BSFC was computed as follows:

$$\omega_{\text{BSFC}} = \sqrt{\left(\frac{\omega\dot{m}_f}{\dot{m}_f}\right)^2 + \left(\frac{\omega P_b}{P_b}\right)^2},$$

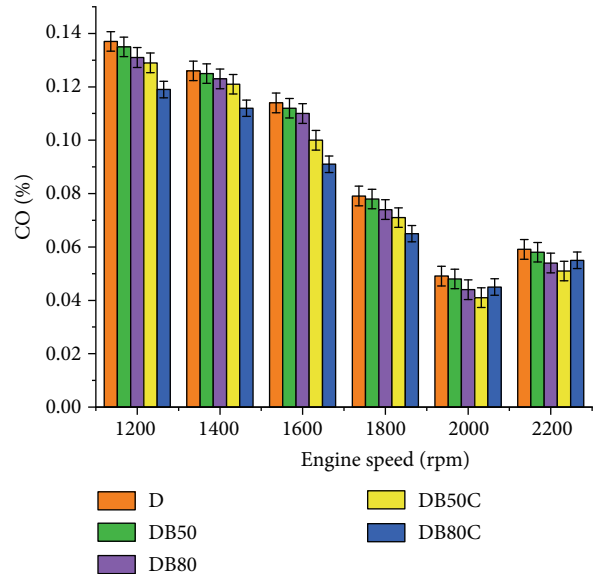


FIGURE 8: CO emissions across various engine speeds (error bars represent the standard deviation ($\pm\text{SD}$) based on three repeated experimental trials under identical conditions).

TABLE 4: Uncertainty, accuracy, and measuring ranges of the measurement instruments.

Parameters	Uncertainty (%)	Accuracies	Measuring ranges
BSFC	$\pm 1 \text{ g/kWh}$	—	—
BP	$\pm 2\%$	$\pm 0.7 \text{ kW}$	0–120 kW
Speed	$\pm 1\%$	$\pm 3 \text{ rpm}$	0–6000 rpm
Temperatures	$\pm 0.5\%$	$\pm 2^\circ\text{C}$	0–2000°C
UHC	$\pm 0.1\%$	$\pm 7 \text{ ppm}$	0–2400 ppm
CO	$\pm 2\%$	$\pm 6 \text{ ppm}$	0–7000 ppm
NO_x	$\pm 0.5\%$	$\pm 5 \text{ ppm}$	0–190 ppm

where $\omega\dot{m}_f$ and ωP_b are the uncertainties in fuel flow rate and BP, respectively. The BSFC uncertainty was found to be $\pm 1 \text{ g/kWh}$. Other instrument uncertainties were expressed as percentages, as shown in Table 4. Using the RSS method, the combined uncertainty of all measured and derived parameters yielded a total uncertainty of 3.24% for the experiment.

$$\omega_{\text{Exp}} = \left[(\text{BSFC}_\omega)^2 + (\text{BP}_\omega)^2 + (\text{speed}_\omega)^2 + (\text{temp}_\omega)^2 + (\text{UHC}_\omega)^2 + (\text{CO}_\omega)^2 + (\text{NO}_X)_\omega \right]^{1/2},$$

$$\omega_{\text{Exp}} = \left[(1)^2 + (2)^2 + (1)^2 + (0.5)^2 + (0.1)^2 + (2)^2 + (0.5)^2 \right]^{1/2},$$

$$\omega_{\text{Exp}} = 3.24\%.$$

3. Results and Discussions

The experimental results are thoroughly analyzed, covering key performance indicators such as specific fuel

consumption and BP in dedicated subsections. Additionally, emission characteristics, including NO_x , CO, and UHCs, are evaluated.

3.1. BSFC. Figure 4 presents the BSFC in grams per kilowatt-hour at various engine speeds (revolutions per minute) for five fuel types: D, DB50, 80% biodiesel–diesel blend (DB80), DB50C, and 80% biodiesel–diesel blend with an additive (DB80C). The general trend observed in the graph shows that BSFC increases with increasing engine speed for all fuel types, indicating that fuel consumption becomes less efficient at higher speeds [35].

At 1200 rpm, BSFC ranges from approximately 240–244 g/kWh, with DB50C and DB80C exhibiting the lowest BSFC, signifying higher fuel efficiency. In contrast, diesel–biodiesel blend (DB80) shows the highest BSFC, indicating lower fuel efficiency. As the engine speed rises to 1400 rpm, the BSFC slightly rises for all conditions, ranging from approximately 241–245 g/kWh. DB50C and DB80C continue to display lower BSFC compared to other fuels, while diesel–biodiesel blend (DB80) remains the least efficient. At 1600 rpm, BSFC further increases, ranging from approximately 240–250 g/kWh. DB50C and DB80C maintain their lower BSFC values, while DB80 has the highest BSFC. At 1800 rpm, BSFC ranges from approximately 250–260 g/kWh, with DB50C and DB80C still showing lower BSFC compared to other fuels, and DB80 exhibiting higher BSFC. When the engine speed reaches 2000 rpm, BSFC increases to a range of approximately 255–265 g/kWh. DB50C and DB80C have lower BSFC values, while DB80 continues to show higher BSFC. At the highest engine speed of 2200 rpm, BSFC reaches its peak values, ranging from approximately 260–270 g/kWh. DB50C and DB80C still exhibit lower BSFC values, while DB80 has the highest BSFC, indicating lower fuel efficiency at this speed.

The enhancement in BSFC observed for the biodiesel blend with carbon nanotubes (DB80C) compared to DB80 without CNTs can be linked to the distinctive characteristics of carbon nanotubes. Acting as a combustion catalyst, CNTs facilitate more efficient fuel oxidation and contribute to an improved combustion rate. This leads to a higher thermal efficiency, resulting in reduced BSFC. Additionally, the high thermal conductivity of CNTs facilitates better heat transfer inside the combustion chamber, further improving energy utilization. These combined effects explain why DB80C exhibits relatively the lowest BSFC compared to other blends, despite DB80 without CNT showing the highest BSFC.

The presence of 50 ppm CNTs in the DB50C and DB80C blends notably influenced the injection and combustion behavior of the fuel. The high surface area and excellent thermal conductivity of CNTs improved the evaporation rate of fuel droplets and shortened the ignition delay period, resulting in more homogeneous combustion. These nanoparticles acted as microcatalytic sites during injection, enhancing atomization and fuel–air mixing, thereby ensuring more efficient energy release during the premixed combustion phase. Consequently, improved heat transfer and faster oxidation reduced localized rich zones within the combustion chamber, minimizing incomplete combustion

products such as CO and UHC. The enhanced combustion temperature and shortened ignition delay also contributed to slightly higher BP and lower BSFC values compared to the blends without CNTs. These findings align with earlier studies reporting that CNT additives facilitate superior combustion kinetics by improving fuel reactivity and spray dynamics within the cylinder [36].

3.2. BP. The BP as a percentage across different engine speeds (revolutions per minute) for five different fuels, such as D, DB50, DB80, DB50C, and DB80C, is shown in Figure 5. The increase in BP is due to improved fuel combustion and more efficient energy conversion, which leads to the production of useful work. It can be concluded that the engine's torque and speed are key factors in determining its total power output. Throughout the engine's speed range, the enhancement in power is explained by the improvement in torque [37].

As engine speed increases from 1200 to 2200 rpm, BP generally increases for all fuel types. This indicates that the engine produces more power at higher speeds. At lower speeds (1200 and 1400 rpm), the BP is relatively low, with values ranging around 14%–18%. As the speed increases to 1600 and 1800 rpm, the BP shows a significant increase, reaching around 18%–22%. At the highest speeds (2000 and 2200 rpm), all fuel types demonstrate their peak BP, with values approaching or slightly exceeding 23%. The differences in BP among the different fuel conditions are minimal, indicating that the type of fuel blend has a less significant impact on power output compared to engine speed. Overall, the graph suggests that engine speed is a critical factor influencing BP, and while biodiesel blends (with and without additives) perform similarly to D in terms of power output, they do not show a distinct advantage or disadvantage in the range of speeds tested.

3.3. NO_x Emissions. Figure 6 presents the NO_x emissions, measured in parts per million, at various engine speeds (revolutions per minute) for five fuel conditions: D, DB50, DB80, DB50C, and DB80C. Generally, NO_x emissions increase with engine speed, peaking at moderate speeds (1400–1600 rpm), and then decreasing at higher speeds (2000–2200 rpm).

At 1200 rpm, NO_x emissions range from approximately 300–500 ppm, with D showing the highest emissions and DB80C the lowest. At 1400 and 1600 rpm, NO_x emissions peak, with D and the biodiesel blends without additives (DB50 and DB80) showing the highest emissions, while DB50C and DB80C show relatively lower emissions. As engine speeds increase further to 1800, 2000, and 2200 rpm, NO_x emissions decrease across all fuel types. By 2200 rpm, NO_x emissions are at their lowest, ranging from approximately 250–400 ppm. Throughout this range, biodiesel blends with additives (DB50C and DB80C) consistently exhibit the lowest NO_x emissions, indicating their effectiveness in reducing NO_x pollution compared to D and biodiesel blends without additives. This trend demonstrates that while engine speed significantly impacts NO_x emissions, the use of

biodiesel and additives can mitigate these emissions, making them a cleaner alternative to D [38].

3.4. UHC Emission. Figure 7 illustrates the UHC emissions, measured in parts per million, at various engine speeds (revolutions per minute) for different biodiesel–CNT fuel blends. The reduction in UHC emissions with biodiesel blends can be attributed to the earlier ignition timing of biodiesel and the longer combustion duration, allowing for more complete fuel oxidation. [39].

As the engine speed rises from 1200 to 1600 rpm, UHC emissions initially rise, peaking around 1600 rpm. At this speed, D exhibits the highest UHC emissions, while biodiesel blends with additives (DB50C and DB80C) show comparatively lower emissions. This trend suggests that at moderate speeds, the combustion process for D is less complete, leading to higher UHC emissions. Beyond 1600 rpm, UHC emissions begin to decrease across all fuel types. At higher speeds (2000 and 2200 rpm), UHC emissions are significantly reduced. Biodiesel blends with additives (DB50C and DB80C) consistently show the lowest UHC emissions at these higher speeds, indicating more complete combustion and better emission profiles compared to D and biodiesel blends without additives. This overall trend highlights the effectiveness of biodiesel, especially when combined with additives, in reducing UHC emissions, particularly at higher engine speeds. The data suggest that biodiesel blends not only enhance combustion efficiency but also contribute to cleaner engine operation by minimizing the release of UHCs.

3.5. CO Emissions. Figure 8 illustrates the CO emissions as a percentage across different engine speeds (revolutions per minute) for D and its blends with biodiesel and CNTs. At lower engine speeds (1200–1400 rpm), CO emissions are relatively high, with values around 0.12%–0.14%. The CO emission levels are minimized when the engine runs at peak load at 2000 rpm. This is likely because the air–fuel mixture reaches a stoichiometric ratio at this speed, promoting more complete fuel combustion and consequently lowering CO emissions [40].

D generally exhibits the highest CO emissions, while biodiesel blends, especially those with additives (DB50C and DB80C), show slightly lower emissions. This trend suggests incomplete combustion at lower engine speeds, leading to higher CO production. As engine speeds increase from 1600 to 2200 rpm, CO emissions decrease across all fuel types. At higher speeds (2000–2200 rpm), CO emissions are significantly reduced, dropping to approximately 0.04%–0.08%. At these higher speeds, DB50C consistently demonstrated the lowest CO emissions, indicating more complete combustion and better emission profiles compared to D, DB50, and DB80. Similar results are shown by Ammar et al. [41] in their study. The overall trend highlights the effectiveness of biodiesel, particularly with additives, in reducing CO emissions and enhancing combustion efficiency, especially at higher engine speeds. This data suggests that biodiesel blends are a cleaner alternative to D, contrib-

uting to lower CO emissions and improved engine performance.

Changes in CO emissions at varying engine speeds are influenced by the air–fuel ratio. At higher speeds, greater air intake improves combustion efficiency, creating a leaner mixture and lowering CO emissions. In contrast, lower engine speeds restrict air intake, which may cause incomplete combustion and increased CO emissions. This trend highlights the significant role of the air–fuel ratio in influencing CO emissions across varying engine speeds.

3.6. Catalytic Role of CNTs in Combustion. CNTs exhibit remarkable catalytic behavior in diesel and biodiesel combustion due to their unique structural and thermal properties [42]. Their large specific surface area and high aspect ratio promote uniform dispersion of fuel molecules, improving atomization and air–fuel mixing within the combustion chamber [43]. CNTs also act as active catalytic sites that facilitate oxidation reactions by enhancing the formation of free radicals such as OH• and O•, which accelerate the breakdown of HC chains during combustion.

Moreover, CNTs possess high thermal conductivity, enabling faster heat transfer and a more uniform temperature distribution in the cylinder [44]. This improved thermal environment supports more complete combustion and reduces ignition delay. The oxygen-containing functional groups on CNT surfaces (especially when mildly oxidized) can further contribute to oxygen donation, improving local oxidation rates and reducing the concentration of incomplete combustion products such as CO and UHC.

In addition, CNTs can lower the activation energy of the oxidation process by providing active reaction sites, similar to metal-based catalysts. These effects collectively enhance combustion efficiency, increase BP, and reduce emissions. Therefore, the catalytic behavior of CNTs is a key factor explaining the improved performance and reduced pollutant formation observed in CNT-blended biodiesel fuels [45].

4. Limitations of the Study

While this study provides significant insights into the synergistic effects of biodiesel and nanomaterials on engine performance and emissions, certain limitations must be acknowledged:

- *Limited scope of nanomaterials:* Only one type of nanomaterial (e.g., CNTs) was tested in this study. Other nanoparticles may yield different results due to variations in thermal conductivity, catalytic behavior, or dispersion stability.
- *Short-term engine testing:* The engine performance and emissions were evaluated under short-duration testing. Long-term durability and deposit formation effects due to biodiesel-nanoparticle blends were not studied and remain an open area for further research.
- *Lack of real-world operating conditions:* Tests were conducted in controlled laboratory conditions. Real-world engine operations, including variable loading,

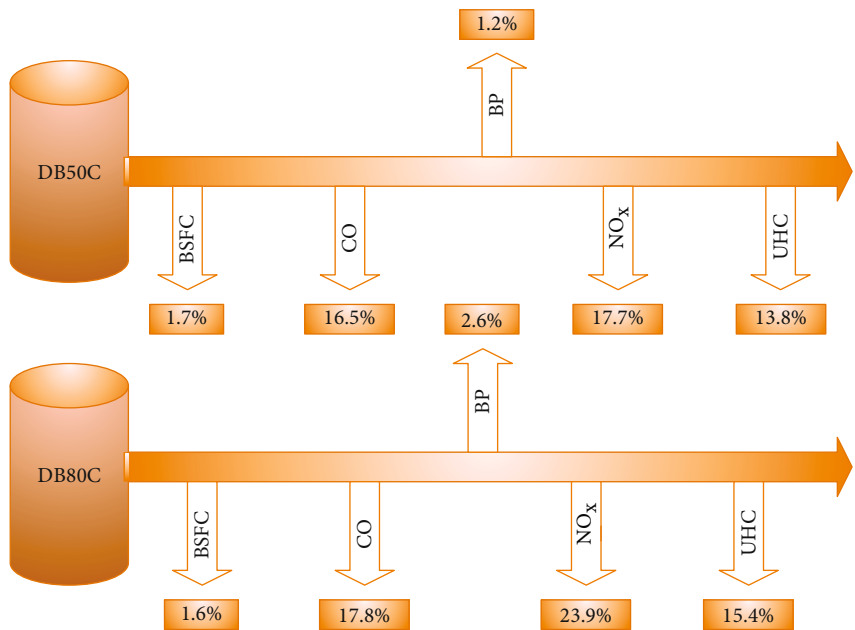


FIGURE 9: Comparison of pure diesel with DB50C and DB80C.

TABLE 5: Statistical analyses of all fuel blends' engine performance and emissions in comparison to pure diesel.

Fuel blends	BP (kW)			BSFC (g/kWh)			CO (%)			UHC (ppm)			NO _x (ppm)		
	p value	F value	Δ (mean values)	p value	F value	Δ (mean values)	p value	F value	Δ (mean values)	p value	F value	Δ (mean values)	p value	F value	Δ (mean values)
DB50	0.0048	608.47	1.956	0.0007	352.49	-7.927	0.0087	6.646	2.354	0.04	245.461	21.546	0.0014	40.165	21.854
DB80	0.0045	657.82	3.458	0.0026	394.07	-11.291	0.0072	6.915	3.649	0.068	237.046	18.499	0.0125	38.284	28.442
DB50C	0.0031	495.03	2.356	0.0019	301.46	-13.458	0.0088	5.451	3.496	0.092	228.381	31.018	0.0079	31.744	25.949
DB80C	0.0035	531.19	7.598	0.0022	295.92	-14.180	0.0079	5.084	3.984	0.053	249.054	36.395	0.0075	42.458	30.496

transient speeds, and different ambient conditions, might influence the actual performance of the fuel blend.

- **Limited emission parameters:** While key emissions such as NO_x, CO, and UHC were measured, other harmful emissions such as PM composition or aldehydes were not analyzed.
- **Economic and environmental assessment:** A comprehensive cost-benefit and life cycle environmental analysis of biodiesel-nanoparticle preparation, usage, and disposal was beyond the scope of this work.

5. Comparison of D With DB50C and DB80C

Figure 9 presents the impact of diesel-biodiesel blends infused with nanoparticles, specifically DB50C and DB80C, on engine performance and emissions. DB50C, which consists of 50 mL of biodiesel with carbon nanotubes, decreases BSFC by 1.7%, CO emissions by 16.5%, NO_x by 17.7%, and UHCs by 13.8%, while enhancing BP by 1.2%. Similarly, DB80C, comprising 80 mL of biodiesel with carbon nanoparticles, leads to a 1.6% reduction in BSFC, a 17.8% drop

in CO emissions, a 23.9% decrease in NO_x emissions, and a 15.4% decline in UHC emissions, along with a 2.6% rise in BP. Overall, both blends contribute to improved engine performance and reduced emissions. DB50C proves more effective in enhancing BP and lowering BSFC, whereas DB80C achieves greater reductions in NO_x and UHC emissions. The integration of carbon nanoparticles into biodiesel blends enhances fuel properties, ultimately improving engine efficiency and reducing emissions.

6. Statistical Analysis of the Experimental Results

Minitab 20.1.3 software was utilized for statistical analysis, including the calculation of *p* values and *F* values to evaluate the significance of results at a 95% confidence level. This analysis assessed the influence of CNTs and biodiesel on diesel engine performance, focusing on parameters such as BP, BSFC, and emissions, including CO, UHCs, and NO_x. Experimental data were used to determine *p* values and *F* values for each parameter. The results showed that *p* values were below 0.05, while *F* values exceeded 0.05, indicating statistically significant variations among the data sets at a

95% confidence level. Table 5 presents a comparative analysis of p values and F values for various fuel blends, conventional diesel, and the average values of BP, BSFC, CO, NO_x , and UHC. The significant discrepancies observed at a 95% confidence level suggest that fuel additives considerably impact engine performance characteristics.

To explore the relationship between independent variables (biodiesel concentration, CNT concentration, and engine speed) and dependent variables (performance metrics and emissions), multiple linear regression models were developed. The analysis revealed that engine speed and CNT concentration had the most pronounced effects on BP, torque, and BSFC. Biodiesel concentration also played a role, particularly in reducing emissions. Standardized regression coefficients were used to rank the influence of each independent variable, with engine speed and CNT concentration emerging as the most significant factors, followed by biodiesel content. The interaction terms indicated that the combined use of biodiesel and CNTs enhanced engine performance more effectively than either component alone. The symbol Δ (mean values) represents the difference between the average values of each parameter for D and various fuel blends. A negative or positive value signifies whether the characteristic for D was lower or higher compared to the other blends. The high F values and corresponding p values below 0.05 confirm the statistical significance of the observed variations.

7. Economic Analysis

An economic assessment was conducted to evaluate the cost-effectiveness of using biodiesel and nanoparticle additives in diesel engines. The analysis considered the fuel cost, additive cost, and fuel consumption rate during engine operation. The baseline fuel (conventional diesel) was compared with a biodiesel blend (e.g., DB50 and DB80) and biodiesel enhanced with nanomaterials (e.g., CNT nanoparticles at 50 ppm concentration). The market prices used in the analysis were as follows:

- *Diesel*: 1.15 USD/L
- *Biodiesel*: 1.35 USD/L
- *CNT nanoparticles*: 150 USD/kg

For DB50, the cost increase per liter is modest, around 3%–5%. When nanoparticles are introduced at a 50-ppm concentration, the cost increases further by approximately 0.4–0.6 cents per liter, depending on the nanoparticle used. However, due to improvements in combustion efficiency and reduced BSFC, the overall cost per kilowatt-hour of energy produced decreases slightly.

In practice, the reduction in fuel consumption (up to 5%) due to better combustion offsets the cost of nanoparticles, making the nanobiodiesel blends economically viable in large-scale applications where fuel efficiency gains are critical. Thus, the economic analysis confirms that biodiesel-nanoparticle blends offer not only environmental bene-

fits but also competitive operational costs under optimized conditions.

8. Conclusions

The study confirms that biodiesel blends, especially those with additives (DB50C and DB80C), offer significant improvements in fuel efficiency and emission reduction compared to D. These blends demonstrate lower BSFC, comparable BP, and substantial reductions in NO_x , UHC, and CO emissions, showcasing their potential as cleaner and more efficient alternatives to conventional diesel fuel.

- DB50C: 1.7% lower BSFC compared to diesel, indicating better fuel efficiency.
- DB80C: 1.6% lower BSFC compared to diesel, demonstrating improved fuel consumption.
- DB50C: 1.2% increase in BP, showing enhanced power output with additives.
- DB80C: 2.6% increase in BP, indicating higher efficiency and power with higher biodiesel content.
- DB50C: 17.7% reduction in NO_x emissions, highlighting effective emission control.
- DB80C: 23.9% reduction in NO_x emissions, demonstrating superior emission reduction with higher biodiesel content.
- DB50C: 13.8% lower UHC emissions, suggesting more complete combustion with additives.
- DB80C: 15.4% lower UHC emissions, indicating significantly reduced UHCs.
- DB50C: 16.5% lower CO emissions, pointing to improved combustion efficiency.
- DB80C: 17.8% lower CO emissions, showing the highest reduction in CO emissions among the tested fuels.

9. Future Research Directions

While this study has highlighted the benefits of biodiesel-nanomaterial blends in improving engine performance and reducing emissions, several areas remain open for further exploration:

- *Long-term engine durability*: Future research should investigate the long-term impacts of nanomaterials on engine wear, deposit formation, and component life to assess real-world applicability.
- *Cost-benefit and lifecycle analysis*: Studies should focus on the economic viability, energy input-output ratio, and lifecycle environmental impact of biodiesel-nanoparticle blends to support commercial scalability.
- *Hybrid fuel systems*: Exploration of biodiesel-nanoparticle combinations with other alternative fuels (e.g.,

hydrogen and methanol) could uncover further synergies for clean combustion technologies.

- *Emissions beyond regulated pollutants:* Research should also examine the effects on unregulated emissions such as particulate number, PAHs (polycyclic aromatic HCs), and N₂O to ensure comprehensive environmental evaluation.
- *AI and machine learning integration:* The integration of data-driven approaches to predict optimal fuel blend performance and emissions profiles under varying conditions offers promising directions.

Nomenclature

AEF	alternative energy fuel
BP	brake power
BSFC	brake-specific fuel consumption
BTE	brake thermal efficiency
CFD	computational fluid dynamics
CO	carbon monoxide
CO ₂	carbon dioxide
CR	compression ratio
D	diesel
DB50	diesel blended with 50% biodiesel
DB80	diesel blended with 80% biodiesel
DB50C	DB50 blended with 50 ppm CNTs
DB80C	DB50 blended with 50 ppm CNTs
EGR	exhaust gas recirculation
IC	internal combustion
MWCNT	multiwalled carbon nanotube
NO _x	nitrogen oxide

Data Availability Statement

The raw performance and emission data supporting the findings of this study are available from the corresponding author upon reasonable request.

Conflicts of Interest

The authors declare no conflicts of interest.

Author Contributions

Sadia Saleem contributed greatly to this work and should be listed as the first author.

Funding

No funding was received for this manuscript.

Acknowledgments

The authors express their gratitude to the administration of the Swedish College of Engineering and Technology, Rahim Yar Khan, for supporting this research endeavor. The authors would also like to acknowledge ChatGPT, which they used to enhance the language of the manuscript.

References

- [1] M. P. GC, B. S. Ajith, A. K. Shettigar, and O. D. Samuel, *Biofuel Production, Performance, and Emission Optimization: A Comprehensive Approach to Modelling and Optimization* (Vol. 2015) (Springer, 2025).
- [2] S. V. Khandal, Ü. Ağbulut, A. Afzal, M. Sharifpur, K. Abdul Razak, and N. Khalilpoor, "Influences of Hydrogen Addition From Different Dual-Fuel Modes on Engine Behaviors," *Energy Science & Engineering* 10, no. 3 (2022): 881–891, <https://doi.org/10.1002/ESE3.1065>.
- [3] A. Azam, A. Naeem Shah, S. Ali, et al., "Design, Fabrication and Implementation of HE-OBCU-EGR Emission Control Unit on CI Engine and Analysis of Its Effects on Regulated Gaseous Engine Emissions," *Journal of King Saud University-Engineering Sciences* 33, no. 1 (2021): 61–69, <https://doi.org/10.1016/J.JKSUES.2019.10.002>.
- [4] M. Çelik, H. Solmaz, and H. Serdar Yücesu, "Examination of the Effects of Organic Based Manganese Fuel Additive on Combustion and Engine Performance," *Fuel Processing Technology* 139 (2015): 100–107, <https://doi.org/10.1016/J.FUPROC.2015.08.002>.
- [5] S. Vellaiyan, "Enhancement in Combustion, Performance, and Emission Characteristics of a Biodiesel-Fueled Diesel Engine by Using Water Emulsion and Nanoadditive," *Renewable Energy* 145 (2020): 2108–2120, <https://doi.org/10.1016/J.RENENE.2019.07.140>.
- [6] A. K. Wamankar and S. Murugan, "Combustion, Performance and Emission of a Diesel Engine Fuelled With Diesel Doped With Carbon Black," *Energy* 86 (2015): 467–475, <https://doi.org/10.1016/J.ENERGY.2015.04.012>.
- [7] M. Annamalai, B. Dhinesh, K. Nanthagopal, et al., "An Assessment on Performance, Combustion and Emission Behavior of a Diesel Engine Powered by Ceria Nanoparticle Blended Emulsified Biofuel," *Energy Conversion and Management* 123 (2016): 372–380, <https://doi.org/10.1016/J.ENCONMAN.2016.06.062>.
- [8] R. D'Silva, K. G. Binu, and T. Bhat, "Performance and Emission Characteristics of a C.I. Engine Fuelled With Diesel and TiO₂ Nanoparticles as Fuel Additive," *Materials Today Proceedings* 2, no. 4–5 (2015): 3728–3735, <https://doi.org/10.1016/J.MATPR.2015.07.162>.
- [9] S. Gumus, H. Ozcan, M. Ozbey, and B. Topaloglu, "Aluminum Oxide and Copper Oxide Nanodiesel Fuel Properties and Usage in a Compression Ignition Engine," *Fuel* 163 (2016): 80–87, <https://doi.org/10.1016/J.FUEL.2015.09.048>.
- [10] S. H. Hosseini, A. Taghizadeh-Alisaraei, B. Ghobadian, and A. Abbaszadeh-Mayvan, "Effect of Added Alumina as Nano-Catalyst to Diesel-Biodiesel Blends on Performance and Emission Characteristics of CI Engine," *Energy* 124 (2017): 543–552, <https://doi.org/10.1016/J.ENERGY.2017.02.109>.
- [11] M. Zhu, Y. Ma, and D. Zhang, "An Experimental Study of the Effect of a Homogeneous Combustion Catalyst on Fuel Consumption and Smoke Emission in a Diesel Engine," *Energy* 36, no. 10 (2011): 6004–6009, <https://doi.org/10.1016/J.ENERGY.2011.08.015>.
- [12] M. S. Ali, A. N. Shah, S. Saleem, et al., "Eco-Friendly Additives: Performance and Emissions Analysis of a Diesel Engine With Jojoba Methyl Ester and CNT Blends," *International Journal of Energy Research* 2025 (2025): 5787065, <https://doi.org/10.1155/ER/5787065>.

[13] J. Maroušek, "Aluminum Nanoparticles From Liquid Packaging Board Improve the Competitiveness of (Bio)Diesel," *Clean Technologies and Environmental Policy* 25, no. 3 (2023): 1059–1067, <https://doi.org/10.1007/s10098-022-02413-y>.

[14] G. Cruz, A. V. S. Silva, J. B. S. Da Silva, R. de Nazaré Caldeiras, and M. E. P. de Souza, "Biofuels From Oilseed Fruits Using Different Thermochemical Processes: Opportunities and Challenges," *Biofuels, Bioproducts and Biorefining* 14, no. 3 (2020): 696–719, <https://doi.org/10.1002/BBB.2089>.

[15] R. N. Vilas Bôas, M. F. Mendes, R. N. Vilas Bôas, and M. F. Mendes, "A Review of Biodiesel Production From Non-Edible Raw Materials Using the Transesterification Process With a Focus on Influence of Feedstock Composition and Free Fatty Acids," *Journal of the Chilean Chemical Society* 67, no. 1 (2022): 5433–5444, <https://doi.org/10.4067/S0717-97072022000105433>.

[16] L. I. Saeed, A. M. Khalaf, and A. B. Fadhil, "Biodiesel Production From Milk Thistle Seed Oil as Nonedible Oil by Cosolvent Esterification–Transesterification Process," *Asia-Pacific Journal of Chemical Engineering* 16, no. 4 (2021): e2647, <https://doi.org/10.1002/APJ.2647>.

[17] D. Singh, D. Sharma, S. L. Soni, et al., "A Comprehensive Review of Physicochemical Properties, Production Process, Performance and Emissions Characteristics of 2nd Generation Biodiesel Feedstock: *Jatropha curcas*," *Fuel* 285 (2021): 119110, <https://doi.org/10.1016/J.FUEL.2020.119110>.

[18] J. Maroušek and A. Maroušková, "Economic Considerations on Nutrient Utilization in Wastewater Management," *Energies* 14, no. 12 (2021): 3468, <https://doi.org/10.3390/EN14123468>.

[19] I. Y. Dharmegowda, L. M. Muniyappa, P. Siddalingaiah, A. B. Suresh, M. P. Gowdru Chandrashekappa, and C. Prakash, "MgO Nano-Catalyzed Biodiesel Production from Waste Coconut Oil and Fish Oil Using Response Surface Methodology and Grasshopper Optimization," *Sustain* 14, no. 18 (2022): 11132, <https://doi.org/10.3390/SU14181132>.

[20] I. Yalagudige Dharmegowda, L. Madarakallu Muniyappa, A. B. Suresh, M. P. Gowdru Chandrashekappa, and N. B. Pradeep, "Optimization for Waste Coconut and Fish Oil Derived Biodiesel With MgO Nanoparticle Blend: Grey Relational Analysis, Grey Wolf Optimization, Driving Training Based Optimization and Election Based Optimization Algorithm," *Fuel* 338 (2023): 127249, <https://doi.org/10.1016/J.FUEL.2022.127249>.

[21] M. Sivakumar, N. Shanmugasundaram, R. Rameshkumar, and M. Syed Thasthagar, "Effects of Pongamia Methyl Esters and its Blends on a Diesel Engine Performance, Combustion, and Emission Characteristics," *Environmental Progress & Sustainable Energy* 36, no. 1 (2017): 269–276, <https://doi.org/10.1002/EP.12492>.

[22] R. Manimaran, T. Mohanraj, and R. Ashwin, "Green Synthesized Nano-Additive Dosed Biodiesel-Diesel-Water Emulsion Blends for CI Engine Application: Performance, Combustion, Emission, and Exergy Analysis," *Journal of Cleaner Production* 413 (2023): 137497, <https://doi.org/10.1016/J.JCLEPRO.2023.137497>.

[23] B. Kanimozhhi, L. Karthikeyan, T. R. Praveenkumar, S. Ali Alharbi, S. Alfarraj, and B. Gavurová, "Evaluation of Karanja and Safflower Biodiesel on Engine's Performance and Emission Characteristics Along With Nanoparticles in DI Engine," *Fuel* 352 (2023): 129101, <https://doi.org/10.1016/J.FUEL.2023.129101>.

[24] K. Brindahdevi, P. T. Kim, M. Vignesh Kumar, C. Govindasamy, A. Anderson, and B. Gavurová, "Enhancing Emission Control and Analyzing the Performance and Combustion Attributes of Vehicular Engines With Spirulina Micro-algae Diesel Ce2O3 Nanoparticles Blends," *Environmental Research* 239, pt. 2 (2023): 117370, <https://doi.org/10.1016/J.ENVRES.2023.117370>.

[25] M. Gülbüm, "Effects of Compression Ratio, Blending Ratio and Engine Speed on Fuel Cost, Performance and Exhaust Emissions of a Diesel Engine Fueled With Bio-Derived Alternative Fuels," *Sustainable Energy Technologies and Assessments* 53 (2022): 102464, <https://doi.org/10.1016/j.seta.2022.102464>.

[26] M. A. Sattar, M. G. Rasul, M. I. Jahirul, and M. M. Hasan, "An up-to-Date Review on the Progress and Challenges of Hydrogen Storage, and Its Safety and Economic Analysis," *Sustain. Energy Fuels* 8, no. 16 (2024): 3545–3573, <https://doi.org/10.1039/D4SE00281D>.

[27] L. Liu, L. Pang, H. Wu, M. Hafeez, and R. Salahodjaev, "Does Environmental Policy Stringency Influence CO2 Emissions in the Asia Pacific Region? A Nonlinear Perspective," *Air Quality, Atmosphere & Health* 16, no. 12 (2023): 2499–2508, <https://doi.org/10.1007/s11869-023-01417-x>.

[28] M. Gülbüm, "Prediction of Exhaust Gas Temperature of a Diesel Engine Running With Diesel Fuel-Biodiesel-1-Pentanol Ternary Blends," in *IOP Conference Series: Earth and Environmental Science*, vol. 1204, no. 1, p. 012002 (IOP Publishing, 2023), <https://doi.org/10.1088/1755-1315/1204/1/012002>.

[29] M. Usman, A. Ali, Z. H. Yamani, and M. N. Shaikh, "Catalytic Pathways for Efficient Ammonia-to-Hydrogen Conversion Towards a Sustainable Energy Future," *Sustain. Energy Fuels* 8, no. 23 (2024): 5329–5351, <https://doi.org/10.1039/D4SE01029A>.

[30] B. Ghorbani, S. Zendehboudi, and Z. A. Afrouzi, "Thermo-Economic Optimization of a Novel Hybrid Structure for Power Generation and Portable Hydrogen and Ammonia Storage Based on Magnesium–Chloride Thermochemical Process and Liquefied Natural Gas Cryogenic Energy," *Journal of Cleaner Production* 403 (2023): 136571, <https://doi.org/10.1016/J.JCLEPRO.2023.136571>.

[31] M. Gülbüm, "Performance, Combustion and Emission Characteristics of a Diesel Engine Fuelled With Diesel Fuel + Corn Oil + Alcohol Ternary Blends," *Environmental Science and Pollution Research* 30, no. 18 (2023): 53767–53777, <https://doi.org/10.1007/s11356-023-26053-x>.

[32] C. Zhu, O. D. Samuel, M. Patel G C, et al., "Enhancing CI Engine Performance and Emission Control Using a Hybrid RSM–Rao Algorithm for ZnO-Doped Castor–Neem Biodiesel Blends," *Case Studies in Thermal Engineering* 74 (2025): 106841, <https://doi.org/10.1016/J.CSITE.2025.106841>.

[33] R. Elumalai and K. Ravi, "Strategy to Reduce Carbon Emissions by Adopting Ammonia-Algal Biodiesel in RCCI Engine and Optimize the Fuel Concoction Using RSM Methodology," *International Journal of Hydrogen Energy* 47, no. 94 (2022): 39701–39718, <https://doi.org/10.1016/J.IJHYDENE.2022.09.169>.

[34] M. Gülbüm, "Effect of Adding Dimethyl Carbonate and Gasoline to Diesel Fuel + Corn Oil Blend on Performance and Combustion Characteristics of a Diesel Engine," *Environmental Science and Pollution Research* 31, no. 27 (2024): 38926–38939, <https://doi.org/10.1007/s11356-023-27121-y>.

[35] G. Anjaneya, S. Sunil, S. Rao K, et al., "Performance Analysis and Optimization of Thermal Barrier Coated Piston Diesel Engine Fuelled With Biodiesel Using RSM," *Case Studies in*

Thermal Engineering 57 (2024): 104351, <https://doi.org/10.1016/j.csite.2024.104351>.

- [36] Z. Zhang, Y. Lu, Z. Qian, and A. Paul Roskilly, "Spray and Engine Performance of Cerium Oxide Nanopowder and Carbon Nanotubes Modified Alternative Fuel," *Fuel* 320 (2022): 123952, <https://doi.org/10.1016/J.FUEL.2022.123952>.
- [37] N. Karimi Abiyazani, V. Pirouzfar, and C. H. Su, "Enhancing Engine Power and Torque and Reducing Exhaust Emissions of Blended Fuels Derived From Gasoline-Propanol-Nano Particles," *Energy* 241 (2022): 122924, <https://doi.org/10.1016/J.ENERGY.2021.122924>.
- [38] M. Nagappan, A. Devaraj, J. M. Babu, et al., "Impact of Additives on Combustion, Performance and Exhaust Emission of Biodiesel Fueled Direct Injection Diesel Engine," *Materials Today Proceedings* 62 (2022): 2326–2331, <https://doi.org/10.1016/J.MATPR.2022.04.114>.
- [39] S. H. Pourhoseini, M. Ghodrat, M. Baghban, and Z. Shams, "Effects of Blending Energetic Iron Nanoparticles in B20 Fuel on Lower CO and UHC Emissions of the Diesel Engine in Cold Start Condition," *Case Studies in Thermal Engineering* 41 (2023): 102658, <https://doi.org/10.1016/J.CSITE.2022.102658>.
- [40] M. Li, Q. Zhang, and G. Li, "Emission Characteristics of a Natural Gas Engine Operating in Lean-Burn and Stoichiometric Modes," *Journal of Energy Engineering* 142, no. 3 (2016): 04015039, [https://doi.org/10.1061/\(ASCE\)EY.1943-7897.0000304](https://doi.org/10.1061/(ASCE)EY.1943-7897.0000304).
- [41] A. Ahmed, A. N. Shah, A. Azam, et al., "Environment-Friendly Novel Fuel Additives: Investigation of the Effects of Graphite Nanoparticles on Performance and Regulated Gaseous Emissions of CI Engine," *Energy Conversion and Management* 211 (2020): 112748, <https://doi.org/10.1016/j.enconman.2020.112748>.
- [42] J. B. Ooi, C. C. Kau, D. N. Manoharan, X. Wang, M. V. Tran, and Y. M. Hung, "Effects of Multi-Walled Carbon Nanotubes on the Combustion, Performance, and Emission Characteristics of a Single-Cylinder Diesel Engine Fueled With Palm-Oil Biodiesel-Diesel Blend," *Energy* 281 (2023): 128350, <https://doi.org/10.1016/J.ENERGY.2023.128350>.
- [43] A. Aboalhamayie, N. Ahmad, Y. Zhang, M. Ghamari, N. Salah, and J. Alshahrani, "An Experimental Evaluation of Thermo-physical Properties of Colloidal Suspension of Carbon-Rich Fly Ash Microparticles and Single-Walled Carbon Nanotubes in Jet-a Fuel and Its Impact on Evaporation and Burning Rate," *Fuel Processing Technology* 266 (2024): 108155, <https://doi.org/10.1016/J.FUPROC.2024.108155>.
- [44] G. Ramasekhar, "Heat Transfer Innovation of Engine Oil Conveying SWCNTs-MWCNTs-TiO₂ Nanoparticles Embedded in a Porous Stretching Cylinder," *Scientific Reports* 14, no. 1 (2024): 1–14, <https://doi.org/10.1038/S41598-024-65740-8;SUBJMETA>.
- [45] M. Sonachalam, V. Manieniyan, R. Senthilkumar, et al., "Experimental Investigation of Performance, Emission, and Combustion Characteristics of a Diesel Engine Using Blends of Waste Cooking Oil-Ethanol Biodiesel With MWCNT Nanoparticles," *Case Studies in Thermal Engineering* 61 (2024): 105094, <https://doi.org/10.1016/J.CSITE.2024.105094>.